

Quantitative MALDI mass spectrometry imaging for exploring cutaneous drug delivery of tofacitinib in human skin

HANDLER, Anne Mette, POMMERGAARD PEDERSEN, Gitte, TROENSEGAARD NIELSEN, Kim, JANFELT, Christian, JUST PEDERSEN, Anders and CLENCH, Malcolm <<http://orcid.org/0000-0002-0798-831X>>

Available from Sheffield Hallam University Research Archive (SHURA) at:

<https://shura.shu.ac.uk/27882/>

This document is the Accepted Version [AM]

Citation:

HANDLER, Anne Mette, POMMERGAARD PEDERSEN, Gitte, TROENSEGAARD NIELSEN, Kim, JANFELT, Christian, JUST PEDERSEN, Anders and CLENCH, Malcolm (2020). Quantitative MALDI mass spectrometry imaging for exploring cutaneous drug delivery of tofacitinib in human skin. *European Journal of Pharmaceutics and Biopharmaceutics*, 159, 1-10. [Article]

Copyright and re-use policy

See <http://shura.shu.ac.uk/information.html>

Title

Quantitative MALDI Mass Spectrometry Imaging for Exploring Cutaneous Drug Delivery of Tofacitinib in Human Skin

Author names and affiliation

Anne Mette Handler ^{1,2,*}, Gitte Pommergaard Pedersen ¹, Kim Troensegaard Nielsen ¹, Christian Janfelt ², Anders Just Pedersen ¹ and Malcolm R. Clench ³

¹ LEO Pharma A/S, Ballerup, Denmark

² Department of Pharmacy, University of Copenhagen, Copenhagen, Denmark

³ Centre for Mass Spectrometry Imaging, Biomolecular Research Centre, Sheffield Hallam University, Sheffield, United Kingdom

Correspondence to: Anne Mette Handler, Department of Pharmacy, University of Copenhagen, Universitetsparken 2, 2100 Copenhagen, Denmark
annemette.handler@sund.ku.dk

Abstract: In skin penetration studies, HPLC-MS/MS analysis on extracts of heat-separated epidermis and dermis provides an estimate of the amount of drug penetrated. In this study, MALDI-MSI enabled qualitative skin distribution analysis of endogenous molecules and the drug molecule, tofacitinib and quantitative analysis of the amount of tofacitinib in the epidermis. The delivery of tofacitinib to the skin was investigated in a Franz diffusion cell using three different formulations (two oil-in-water creams, C1 and C2 and an aqueous gel). Further, *in vitro* release testing (IVRT) was performed and resulted in the fastest release of tofacitinib from the aqueous gel and the lowest from C2. In the *ex vivo* skin penetration and permeation study, C1 showed the largest skin retention of tofacitinib, whereas, lower retention and higher permeation were observed for the gel and C2. The quantitative MALDI-MSI analysis showed that the content of tofacitinib in the epidermis for the C1 treated samples was comparable to HPLC-MS/MS analysis, whereas, the samples treated with C2 and the aqueous gel were below LOQ. The study demonstrates that MALDI-MSI can be used for the quantitative determination of drug penetration in epidermis, as well as, to provide valuable information on qualitative skin distribution of tofacitinib.

Keywords: Cutaneous drug delivery, skin, tofacitinib, mass spectrometry imaging, skin penetration, skin permeation, MALDI-MSI, *in vitro* release testing, HPLC-MS/MS

1 Introduction

Mass spectrometry imaging (MSI) is a family of techniques for targeted and non-targeted imaging analysis enabling visualization of the distribution of multiple compounds within the same experiment. In pharmaceutical skin research, the compounds of interest could be drug molecules, excipients, metabolites, biomarkers or endogenous molecules such as cholesterol, ceramides etc. Previously, MSI has mainly been used for qualitative assessment of the distribution of different molecules in a tissue sample. However, the technique has quickly gained popularity due its non-targeted approach, which has resulted in an increasing demand for adding a quantitative component to the qualitative MSI data. For Matrix-Assisted Laser Desorption Ionization Mass Spectrometry Imaging (MALDI-MSI), multiple methods to perform quantitative analysis have been developed to solve the challenges, which are inherent for this analytical technique. The challenges comprise of spatial variations in the ionization of the analyte caused by inhomogeneity in matrix deposition and changes in sample composition. Further, tissue binding of the analyte in the sample (e.g. protein or lipid binding) complicates the quantitative analysis and makes it difficult to correlate the calibration curve to the concentrations of the analyte in the sample [1]. Although MSI as a field has existed for more than 20 years, quantitative mass spectrometry imaging (qMSI) is still in its infancy, and unlike in traditional bioanalysis employing HPLC-MS, there is not yet an established consensus on how to construct calibration curves and assess tissue concentrations. The developed methods can be grouped in three categories: “in-tissue” where the calibration curve is established using drug-spiked homogenate, “in-solution” where the calibration standard is deposited on the glass slide next to the sample and “on-tissue” where the calibration standards are deposited on or beneath the sample section [2]. An “in-solution” method was developed by Hamm *et al.*. In this method, the calibration standards were deposited on a clean glass slide, and the signal of the calibration standards were correlated to the drug-treated tissue by use of the tissue extinction factor, TEC [3]. The TEC factor was established by spraying the analyte onto a control tissue and calculate the ratio of the ion signal in a region of the tissue to the ion signal achieved on the clean glass slide. The TEC approach anticipates that the same interactions are present by spraying the analyte on top of the skin as the interactions in drug-treated skin. Other studies have shown that normalizing to a standard which has been sprayed onto the sample with the matrix solution may not fully mimic the interactions in the skin since there is a risk of the standard to co-crystallize with the matrix compound rather than interact with the skin and hence result in an inadequate

normalization [4,5]. To overcome this, several studies have investigated how the application of the standard either beneath or on top of the skin affects the generation of the standard curve [1]. By use of an acoustic spotter, Chumbley *et al.*, found that the best correlation was achieved by spotting the standard on top of the sample before applying the matrix [4], whereas, the best correlation according to Pirman *et al.* was achieved when spraying the standard onto the glass slide before mounting the sample and applying the matrix [6]. Thus, the means for generating standard curves remains inconclusive. Another approach is to create a mimetic tissue model where the relevant biologic matrix is homogenized and spiked with a known concentration of the drug standard [7]. This approach may be more time consuming for smaller analyses than deposition of droplets for establishing a calibration array, whereas, for larger studies, where multiple sections can be made from the same block of mimetic tissue, it may be more feasible and result in less variation than manually spotted droplets where variations in droplet deposition may affect the volume and area covered by the droplet [8]. Finally, an example of an on-tissue approach was developed by Russo *et al.* using an acoustic microspotter to achieve droplets in the picoliter range with reproducible spot sizes [9]. The microspotter was used to establish a calibration array by applying small droplets of different concentrations of the analyte on the epidermal layer of a 3D living skin equivalent model. To adjust for changes in ionization efficiency caused by changes in sample composition and matrix deposition, a stable isotope labelled version of the analytes was used as internal standard (IS). The IS was added to the calibration standards, such that the ion signal of the drug molecule could be normalized to the ion signal of the IS. On the drug treated samples, the IS was spotted in the same concentration as used for the calibration standards with the same purpose of normalizing the signal to encounter differences in analyte-matrix ratio and skin composition.

In this study, the delivery of the model drug molecule, tofacitinib to the skin was investigated from three different formulations using the on tissue MALDI-qMSI method where a calibration array was established by the use of a microspotter [9]. The three formulations consisted of an aqueous gel and two oil-in-water creams based on different emulsifiers and components to provide structure. The qMSI results of the epidermal content of tofacitinib were compared to the content of tofacitinib in epidermis extracts measured by HPLC-MS/MS. The penetration to the dermis and permeation to the receptor media were measured using HPLC-MS/MS to provide a more detailed investigation of the skin penetration and permeation. The penetration is here defined as the passage of molecules into the skin whereas

permeation is defined as the passage of molecules through the skin. The model drug molecule, tofacitinib is a Janus kinase (JAK)-inhibitor and has previously been in clinical phase 3 trials for oral treatment of psoriasis [10–12]. Selected physicochemical properties of tofacitinib are listed in table 1.

2 Materials and Methods

Tofacitinib (98 %) purchased from PharmBlock, Inc. (Hatfield, PA, USA) and [$^{13}\text{C}_3^{15}\text{N}$]-tofacitinib (98 %) from Alsachim (Illkirch Graffenstaden, France). Acetonitrile, methanol, ethanol, formic acid and ammonium acetate were purchased from Merck KGaA (Darmstadt, Germany). Propanolol, Dulbecco's phosphate buffered saline (DPBS), bovine serum albumin (BSA), citric acid, Alpha cyano-4-hydroxycinnamic acid, phosphorus red, haematoxylin and xylene substitute were purchased from Sigma-Aldrich (Copenhagen, Denmark). Eosin and Pertex mounting medium were purchased from Leica Biosystems Nussloch GmbH (Nussloch, Germany). Milli-Q water was obtained from a Direct-Q 5 UV Remote Water Purification System (Billerica, MA, USA).

2.1 Characterization of formulations

2.1.1 Formulations

The three different formulations were prepared by homogenously suspending 10 mg/g tofacitinib in the vehicle using a pestle and mortar. The aqueous gel consisted of a base of water and glycerol and hydroxyethylcellulose used as a gelling agent. C1 contained an aqueous phase of water and glycerol and a blend of monoglycerides as disperse phase, macrogol-40-stearate as emulsifying system and carbomer as stabilising agent. C2 contained an aqueous phase of water, glycerol and sorbitol and a disperse phase of liquid paraffin, and an emulsifier system of polysorbate 80, cetostearyl alcohol and glycerol monostearate.

2.1.2 *In vitro* release testing (IVRT)

IVRT of tofacitinib from the three formulations was performed using a Hanson Vision Microette automated diffusion test system (Teledyne Hanson Research, Chatsworth, CA, USA) in modified Franz diffusion cells with a synthetic membrane Tuffryn® 0.45 μm (Pall, Portsmouth United Kingdom). The experiment was performed with six replicates of each formulation. To maintain sink condition in the receptor compartment during the experiment, degassed 50:50 v/v% ethanol (EtOH):H₂O was used as receptor media. The diffusion cells consisted of a 265 μl donor compartment and a 7 ml receptor compartment equipped with magnetic helix stirring at 600 rpm. The temperature was maintained at 32°C during the

experiment.

Before initiating the experiment, the membranes were soaked for 30 minutes in the receptor media and the diffusion cells were filled with receptor media and left to equilibrate for 30 minutes. 265 μL of the formulations were pipetted into the donor compartments using a positive displacement pipette and the membranes were subsequently mounted onto the donor compartment. The receptor compartment was filled with the degassed receptor media and clamped together with the donor compartment. It was ensured that air bubbles were removed before initiation. 500 μL receptor media were sampled after 15, 30, 45 minutes, 1, 2, 3, 4, 5, 6, 8, 10, 14, 20 and 24 hours and replaced by fresh receptor media.

The release rate and flux were determined as described in the SUPAC-SS using Higuchi kinetics for semisolid formulations (square root t kinetics) by plotting the amount released per area ($\mu\text{g}/\text{cm}^2$) as a function of the square root of time ($\text{min}^{1/2}$) [13]. A linear regression line was plotted and the slope ($\mu\text{g}/(\text{cm}^2 \text{ min}^{1/2})$) represented the flux.

2.1.3 HPLC-UV analysis of IVRT samples

The sampled receptor media from IVRT were injected directly into a Dionex 3000 Ultimate HPLC system (Thermo Fisher Scientific Inc., Waltham, MA, USA) equipped with a PDA detector, without further sample preparation. The standards were prepared using a diluent consisting of 50:50 v/v% of EtOH:H₂O. An Agilent Zorbax Eclipse Plus C18 column (2.1x50 mm, 1.8 μm) was operated at 40 °C, an injection volume of 1 μL and a flow rate of 0.4 mL/min. Mobile phase A (10 mM ammonium acetate in 10:90 v/v% ACN:H₂O) and mobile phase B (10 mM ammonium acetate in 80:20 v/v% ACN:H₂O) were used with a programmed gradient of 0-4.5 minutes 0-45% (B); 4.5-5.5 minutes 45-70% (B); 5-7 minutes: isocratic gradient 0% (B). A wavelength of 283 nm was used for detection. The limit of detection (LOD) was experimentally determined to be 1.0 $\mu\text{g}/\text{mL}$ by preparing standards close to LOD.

2.2 Ex vivo penetration and permeation

2.2.1 Preparation of skin

Excess full-thickness skin removed in plastic surgery was received from Herlev Hospital (Herlev, Denmark) upon written informed consent of the donor. Skin samples were donated by three different donors; abdominal skin from two female donors (24 and 62-years old) and arm skin from a female donor (47-years old). The surgically removed skin was prepared by removing subcutaneous fat and frozen to -20 °C until the day of the experiment.

2.2.2 Franz diffusion cell study on human skin

On the day of the experiment, skin explants of 38 mm diameter were punched out and fixed into a Franz diffusion cell setup (PermeGear, Inc., Hellertown, PA, USA) with a diffusion area of 3.1 cm². The skin explant originated from three different donors described in section 2.2.1. The cells were filled with isotonic saline water. After 30 minutes, the saline water was exchanged with 4 w/w% BSA in DPBS and the cells were left to equilibrate for 45 minutes. The temperature on top of the skin was maintained at 32 °C during the experiment. After 45 minutes, 20 µL of the formulations were applied on top of the skin using a pipette. The experiment was performed in triplicate. The MALDI-MSI analysis was performed on skin treated with the three different formulations for 5 and 24 hours. Hence, three Franz diffusion cells for each of the three different formulations were prepared for the 5-hour treatment and another three Franz diffusion cells for the 24-hour treatment. The skin explants used in the set of three Franz diffusion cells used skin originating from two out of the three included skin donors to get an insight into the variation between two skin explants from the same skin donor. The skin treated with C1 originated from the abdominal skin of a 24 and 62-years old woman, whereas, the gel and C2 treated skin originated from arm skin of a 47-years old woman and abdominal skin of a 62-years old woman. The receptor media (0.5 mL) was sampled after 1, 3, 5, 7, 22 and 24 hours and replaced with fresh receptor media. For cells discontinued after 5 hours for MALDI-qMSI analysis, the receptor media were sampled after 1, 3 and 5 hours to provide the same conditions.

At the end of the experiment, the receptor media was collected and weighed (approximately 10-11 g). 0.5 mL of the receptor media was transferred to an Eppendorf tube for HPLC-MS/MS analysis. The skin was carefully removed from the diffusion cells and tape-stripped twice with Transpore (3M, St. Paul, MN, USA) using a pressure applicator with an applied pressure of approximately 1.3-1.4 kg. Subsequently, the skin was tape-stripped six times with D-Squame (CuDerm Corporation, Texas, USA) tape without the use of a pressure applicator. A 10 mm punch biopsy was taken from the skin explant and the 10 mm biopsy was turned upside down and a 6 mm punch biopsy was made from the dermal side. The 6 mm biopsy was transferred to an Eppendorf tube and left on a 55 °C water bath for 5 minutes to heat-separate epidermis from dermis. The epidermis was carefully removed from dermis and the epidermis and dermis were transferred to individual tubes suited for a bead ruptor (vials containing small grinding balls of different sizes). To assess the weight of the epidermis and dermis, the tubes suited for a bead ruptor were weighed before and after the sample was

collected. 600 μ L cold 50:50 v/v ACN:H₂O was added to the tubes. 6 mm punch biopsies were made for the MALDI-MSI analysis and transferred to a tube before snap freezing in liquid nitrogen. The samples were stored at -80 °C.

Sink conditions were upheld during the experiment and were defined as 10% of the saturation solubility of the drug molecule in the receptor media [14].

2.3 HPLC-MS/MS bioanalysis of dermis, epidermis and receptor media

The dermis and epidermis samples were homogenized using a Bead Ruptor 24 (Omni International, Kennesaw, GA, USA) operated in 5 cycles of 20 s with a 1-minute delay between each cycle with cooling provided by an Omni BR-Cryo Cooling Unit. The samples were added 400 μ L 50:50 v/v% ACN:citrate buffer (pH = 4) and centrifuged at 4000 rpm for 30 minutes. 50 μ L of the supernatant was transferred to a 96-deep well plate and 150 μ L ACN with 5 nM propranolol as internal standard (IS) was added to precipitate proteins. The 96-deep well plate was centrifuged at 4000 rpm for 30 minutes and the samples were now ready for HPLC-MS/MS analysis. The receptor media were prepared for HPLC-MS/MS analysis by mixing 100 μ L of the receptor media with 300 μ L of ACN containing propranolol as an IS. From the mixture 120 μ L was transferred to a 96 deep well plate and centrifuged at 4000 rpm for 10 minutes. The UHPLC-MS/MS system consisted of a Sciex API5500 triple quadrupole mass spectrometer (Framingham, MA, USA) equipped with a Shimadzu prominence UHPLC pump (LC-30AD, Kyoto, Japan) using a Shimadzu autosampler (SIL-20AC, Kyoto, Japan)). The analytes were separated by a Waters C18 T3 HSS (50 \times 2.1 mm, 1.8 μ m) column operated at 60 °C and mobile phases consisting of 10 mM ammonium acetate buffer + 0.1% formic acid (10:1: 89) and 0.1% formic acid in acetonitrile. A programmed gradient was used: 0.0–0.1 min: isocratic at 1% (B); 0.1–0.6 min: 1–100% (B); 0.6–1.6 min: isocratic at 100% (B); 1.6–1.8 min: 100–1% (B); and 1.8–2.5 min: isocratic at 1% (B). The injection volume was 3 μ L and the flow rate was 0.6 mL/min. The mass spectrometer was operated in positive ion mode with electrospray ionization and tofacitinib was quantified using the transition 313.2/149.0. The LOD for tofacitinib was determined as 3 times the noise to 12 ng/g for the skin extracts and 0.6 ng/g for the receptor media where the noise was determined as the background in the mass spectrum of a blank.

2.4 MALDI-qMSI

2.4.1 Cryo-sectioning

The skin samples were cryo-sectioned into 12 µm thick sections without the use of embedding (Leica CM1950, Leica Biosystems Nussloch GmbH, Nussloch, Germany). The samples were mounted to a cork ring using ice before attaching the cork ring to the sample holder. The sectioning was performed at -18 to -20 °C. Multiple samples were thaw-mounted onto the same polylysine glass slide allowing each slide to comprise of cross-sections of a control, a vehicle-treated and two to three tissue sections treated with the formulation, all from the same donor. The polylysine slides were packed in boxes of two slides and put into a sealed bag to avoid dislocation of analytes when thawing the samples on the day of the analysis. The samples were stored at -80 °C.

2.4.2 Microspotting of standards

An acoustic robotic spotter (Portrait 630, Labcyte Inc., Sunnyvale, CA, USA) was used to apply the calibration standards. The standard solutions were prepared in concentrations of 1500, 1000, 500, 100, 50, 10 and 1 µg/mL in 50:50 v/v% MeOH:H₂O. To each standard, IS was added to obtain a concentration of 100 µg/mL. The standard was microspotted onto control tissue in 20 cycles of 170 picoliters each, such that a total volume of 3.4 nL was deposited for each calibration spot. The samples treated with the formulation and the vehicle were microspotted with 3.4 nL of 100 µg/mL IS at the locations on the samples where quantification was desired. A total of 9 spots were deposited in the epidermis of each sample.

2.4.3 Sublimation

300 mg of CHCA was distributed homogenously across the bottom of a sublimation chamber. The glass slide was attached to the bottom of the flat top of the sublimation chamber. The sublimation apparatus was assembled using an O-ring and a vacuum was applied. The vacuum was stabilized around $2.5\text{--}2.7 \times 10^{-2}$ Torr and ice-cold water was poured into the top of the sublimation chamber. The chamber was placed on sand heated to approximately 180 °C. A layer of 0.1-0.2 mg/cm² CHCA was applied to the polylysine slide within 3 to 4 minutes.

2.4.4 MALDI-MSI

A Waters MALDI HDMS Synapt G2 mass spectrometer (Waters Corporation, Manchester, U.K.) equipped with a neodymium:yttrium aluminum garnet (Nd:YAG) laser operated at 1 kHz was used to analyze the samples. The analysis was carried out in full scan “sensitivity”

mode with a pixel size of 60 μm and a mass range of m/z 100–800, (resolution 10 000 fwhm). The laser energy was set to 270 (arbitrary units). The RAW-files were converted to imzML files using HDI Imaging Software version 1.4 (Waters Corporation, Manchester, U.K.). The imzML files were subsequently visualized in msIQuant version 2.0.1.14 [15]. The MALDI images are presented as the ion signal normalized to the total ion count (TIC). Tofacitinib was visualized as its hydrogen adduct at m/z -value 313.2 and IS as its hydrogen adduct at m/z -value 317.2. The MALDI images were acquired with a bin width of ± 0.050 Da.

2.4.5 H&E staining

After the MALDI-MSI analysis, the skin sections were stained using haematoxylin and eosin (H&E) staining. The staining was performed by submerging the slide for three minutes in 100% EtOH, and thereafter in 95%, and 70% EtOH solutions. Subsequently, the slide was washed in Milli-Q water for 2 minutes before the slide was immersed for 10 minutes in filtered Meyer's hematoxylin. Then, the slide was washed in running tap water for 3-5 minutes before dehydrating the slide for 3 minutes in 70% EtOH, and then in 95% EtOH solutions. The slide was submerged for 1 minute in filtered eosin and washed for 3 minutes in 95% EtOH solution, and another 3 minutes in a new chamber of 95% EtOH solution. Subsequently, the slide was washed in 100% EtOH for 3 minutes before being transferred to another solution of 100% EtOH for 3 minutes. Thereafter, the slide was submerged twice in two chambers of xylene substitute for 5 minutes each and finally mounted using the mounting medium, Pertex. The optical images were acquired using an Olympus BX60 microscope.

2.4.6 Quantification using MALDI-MSI

In msIQuant, the microspotted standards on tissue were interrogated by the ecliptic or polygonic tool depending on the shape of the microspotted droplet. From the interrogated region, the average signal of IS and tofacitinib were extracted using a bin width of ± 0.050 Da. The standard curve for each MALDI analysis was plotted as the ratio of tofacitinib and IS as a function of the spotted mass of tofacitinib divided by the area (ng/mm^2). The ratio between the average signal of tofacitinib and IS is later designated as the *mean intensity ratio*. The extracted concentrations in ng/mm^2 were converted to $\mu\text{g}/\text{g}$ tissue by calculating the volume of the tissue. The volume of the tissue was determined by multiplying the area of 1 mm^2 with a skin section thickness of 0.012 mm ($12 \mu\text{m}$). The volume, 0.012 mm^3 was multiplied with the density of the skin set to $1 \text{ mg}/\text{mm}^3$ resulting in 0.012 mg tissue. Hence, the extracted concentration in ng/mm^2 could be converted to ng/mg , which is the same unit as

$\mu\text{g/g}$, by dividing with 0.012 mg of tissue in 1 mm^2 . For the individual biological replicate, the mean of all concentrations determined for each of the microspots was calculated and compared to the HPLC-MS/MS data. In the MALDI images, it was observed that a fraction of IS was not isotopically labelled. To account for this contribution, a correction factor was introduced based on the microspots of the IS applied on the skin treated with the vehicle. The correction factor was determined by extracting the *mean intensity ratio* of tofacitinib and IS to calculate the contribution as a concentration in ng/mm^2 . The correction factor was subtracted from the concentrations determined on the tofacitinib-treated skin.

LOD and LOQ were determined for the experiments by calculating the standard deviation of the y estimate, s_y based on the standard curve of the three MALDI-MSI datasets used for the quantification of tofacitinib. LOD was calculated as $3s_y/\text{slope}$ and LOQ as $10s_y/\text{slope}$. The LOD was determined to be 0.60 ng/mm^2 corresponding to $50.3\text{ }\mu\text{g/g}$ and a LOQ of 2.01 ng/mm^2 corresponding to $168\text{ }\mu\text{g/g}$.

2.5 Statistical analysis

Non-parametric Mann-Whitney U test and non-parametric Kruskal-Wallis one-way analysis of variance followed by multiple comparison tests were performed. For qMSI, Grubbs outlier test was carried out to exclude outlying concentrations achieved from the individual microspots. All statistical analyses were performed using GraphPad Prism 8 for Windows, GraphPad Software, La Jolla California USA, www.graphpad.com. Two-tailed p-values below 0.05 were considered statistically significant. The data were presented as mean \pm standard deviation (SD).

3 Results and Discussion

3.1 Characterization of formulations

3.1.1 *In vitro* release testing

IVRT was performed for 24 hours. Within the first six hours, steady-state condition was assumed to be upheld and the fluxes for the three formulation were calculated using square root t kinetics [13]. In figure 1, the amount of tofacitinib in the receptor compartment per area ($\mu\text{g/cm}^3$) is depicted as the function of time ($\text{min}^{1/2}$).

The flux, lag time and amount of released tofacitinib after 6 hours for each of the three formulations are presented in table 2. The largest flux was obtained for the gel and the lowest

for the C2 cream. A significant difference in the amount of tofacitinib released after 6 hours was found between the gel and the C2 cream ($p=0.0003$).

3.2 Ex vivo penetration and permeation

3.2.1 HPLC-MS/MS analysis of tofacitinib in epidermis, dermis and receptor media

The penetration and permeation of tofacitinib are visualized in figure 2a and b. The penetration data showed the highest accumulated amount of tofacitinib in epidermis and dermis was achieved for the C1 cream after 5 hours with a recovered dose of $1.9 \% \pm 0.2\%$ ($n=3$) and after 24 hours with a recovered dose of $6.8 \% \pm 4.2\%$ ($n=3$). The lowest recovered dose in dermis and epidermis was measured for the gel-treated samples where tofacitinib was only detected in the epidermis with a recovered dose of $0.8 \% \pm 0.4 \%$ ($n=3$) after 24 hours. One data point of the tofacitinib concentration in the epidermis for a sample treated with the C2 was removed due to insufficient tape-stripping which resulted in 22 times higher recovered tofacitinib content in the epidermis than the other two biological replicates. The recovered dose of tofacitinib in dermis and epidermis for the C2-treated samples after 24 hours was determined to $1.4\% \pm 0.2\%$ ($n=2$, after the exclusion of outlier). At 5 and 24 hours, a significant difference was found between the gel and the C1-treated samples ($p_{5 \text{ hours}}=0.0338$ and $p_{24 \text{ hours}}=0.0219$), whereas, the difference between the other formulations showed to be non-significant.

In contrast to the penetration data, the permeation data in figure 2b showed that the highest recovered amount of tofacitinib was achieved for samples treated with the aqueous gel and the C2 cream. For the samples treated with C1, tofacitinib was only detected in the receptor media for one cell after 24 hours with a recovered amount of 1.3 %. For the samples treated with C2 and the aqueous gel, tofacitinib was detected after 24 hours in two out of three cells with a recovered amount of $7.4\% \pm 7.9\%$ ($n=3$) for the samples treated with the C2 and $6.9 \% \pm 6.1\%$ ($n=3$) for the samples treated with the aqueous gel.

3.2.2 MALDI-MSI analysis of tofacitinib distribution

The epidermal thickness was determined for the skin donors with an average thickness of 40-60 μm measured from the H&E stained skin sections. An epidermal marker found at m/z 365.3 and tentatively assigned to a cholesterol-related peak that had undergone fragmentation in the ion source resulting in a proposed structural formula of $\text{C}_{27}\text{H}_{40} [\text{M}+\text{H}]^+$. The epidermal marker found in the MALDI images had a similar appearance as the epidermis from the H&E

staining with a thickness of about 1-2 pixels (relative to 60-120 μm) as seen in figure 3. Thus, the epidermal marker visually appears slightly thicker on the MALDI images than the H&E staining. However, with a pixel size of 60 μm , there is an uncertainty associated with the thickness of the epidermal marker compared to the high resolution of the microscopic examination of the H&E stained tissue. The spots of IS had an approximate diameter of three pixels relative to a diameter of approximately 180 μm . This was comparable to the microspot diameter of approximately 0.16 mm (area of $0.019 \pm 0.0027 \text{ mm}^2$ and $0.021 \pm 0.0028 \text{ mm}^2$) obtained by Russo *et al.* where the diameter was optically measured on microspots of the gentian violet dye on a living skin equivalent [9].

3.2.3 qMSI

The normalization of the mean intensity of tofacitinib to the IS improved the linearity of the standard curves as seen in figure 4, where the mean intensity of tofacitinib and the *mean intensity ratio* of tofacitinib and IS were plotted as a function of the concentration of the microspotted droplets. Implementation of internal standards in qMSI is a widely used method to compensate for variabilities in sample preparation and the matrix-analyte ratio [8]. An important consideration when using an internal standard for qMSI is to select an IS that resembles the analyte in terms of molecular weight, solubility and similar ionization efficiency [1]. In this case, a stable isotope of the analyte was chosen and demonstrated to be efficient for improving the linearity of the standard curve. Similar observations have been reported, for instance, by Källback *et al.* where normalization to a stable isotope standard was performed by depositing the analyte on top of control tissue before spraying the matrix solution containing the deuterated standard on the surface of the sample [16].

For each MALDI analysis, a new standard curve was prepared to compensate for day-to-day variation in terms of matrix application and instrumentation. The linear fit, R^2 showed a fit of 0.99-1.00 for the three datasets included in the quantification. A comparison of the three calibrations showed minimal inter-day variation when the internal standard was used for calibration. A LOD of 0.60 ng/mm² relative to 50.3 $\mu\text{g/g}$ and a LOQ of 2.01 ng/mm² relative to 168 $\mu\text{g/g}$ were determined based on the calibration data.

The results from the HPLC-MS/MS analysis showed that the content of tofacitinib recovered in the epidermis was lower in the samples treated with gel and C2 compared to the samples treated with C1 (figure 2a). This was mirrored in the MALDI-qMSI data, where the signal of

tofacitinib in most samples treated with gel and C2 were below LOQ and often also below the LOD. However, in a few of the microspots applied to the samples treated with gel or C2, the signal of tofacitinib was above the LOQ and quantification in these microspots was possible. In figure 5, a sample treated with C2 and a sample treated with the aqueous gel are presented; the arrows mark the IS spots where the concentration of the permeated amount of tofacitinib is high enough to be quantified. In these two spots, a concentration of 0.40 mg/g for the samples treated with C2, and 0.47 mg/g for the samples treated with the gel were obtained. The microspots provide a quantitative measure in the applied spots, however, in case of inhomogeneous drug penetration, it is important to apply enough microspots to make an accurate measure of the overall concentration in the epidermis. In this case, low penetration of tofacitinib resulted in an overall quantity of tofacitinib in the epidermis below LOQ for the sample treated with the gel and C2.

For the samples treated with C1, the epidermal content of tofacitinib in the MALDI images was above LOQ and in figure 6 MALDI images of a sample treated with C1 for 5 and 24 hours are shown. The MALDI images of the sample show the epidermal marker, IS and tofacitinib overlaid with the H&E stain. In the images, tofacitinib was observed in the epidermis and upper dermis at 5 and 24 hours.

In figure 7, the concentrations for each microspot are presented with the contribution from the IS for each biological replicate at 5 and 24 hours separated by a dotted line (n=3). One of the biological replicates treated with C1 showed no signal of tofacitinib and was therefore annotated in the figure as below LOD. A few of the microspots were excluded from the quantification due to deposition outside the epidermis which was visually determined from colocalization of the epidermal marker at m/z 365.3. In figure 7, a rather large variation between the microspots was observed for some of the biological replicates, and it was especially pronounced for the samples collected after 24 hours. The observed variation between the microspots could indicate heterogeneous skin penetration which may be caused by biologic variation and skin appendages. The delivery of other small molecules were studied by Barry *et al.* and D'Alvise *et al.* [17,18]. They both suggested that the absorption of these compounds occurred via the appendageal pathway as it was primarily located around hair follicles present near the epidermis [18]. Comparing this to the data obtained for tofacitinib here, the skin distribution indicates a different route of penetration as tofacitinib was primarily observed in the epidermis and not co-distributed with the hair follicles which can be observed in figure 6. This could also be ascribed to limited

sensitivity preventing the detection of tofacitinib at the hair follicles, even if it were present, but another MSI study of tofacitinib (using a different MSI instrumentation and method) suggest likewise that hair follicles do not play a significant role in the delivery of this drug molecule with the used drug delivery systems [19]. Here, additional parameters such as differences in physicochemical properties of the drug molecule and the drug delivery system may affect the skin penetration, as well as, differences in the MALDI-MSI instrumentation and ionization efficiencies of the molecules which affect the sensitivity of the analysis. The skin penetration of tofacitinib has previously been studied using MALDI-MSI where other formulations and dosing were applied, and here tofacitinib was also observed with the highest abundance in the epidermis and the intensity of tofacitinib in dermis being dependent on the applied formulation [20,21]. In line with previous observations, tofacitinib was primarily located in the epidermis in the present study with only a few small clusters scattered across the dermis. A direct comparison between the studies can, however, not be performed as the differences in the experimental setup such as the amount of tofacitinib dosed in the study, the drug delivery system applied, the skin tissue, as well as, the MALDI instrumentation influence the results.

Mean intensities of tofacitinib and IS were extracted and the contribution from the non-labelled impurity of the IS was subtracted. In figure 8, the content in each sample treated with the C1 is compared to the adjacent biopsy analysed by HPLC-MS/MS. At 5 hours, one of the biological replicates analysed by qMSI was below LOQ and, therefore, not included in the figure. No statistical difference was observed between the means at 24 hours ($p=0.70$) for the quantitative data obtained using HPLC-MS/MS and MSI. However, it should be noted that the diameter of the microspots of 180 μm was larger than the thickness of the epidermis of about 60 μm which resulted in an actual quantification of the epidermis and the upper layers of the dermis. Therefore, when the measured quantities by MALDI-qMSI were compared with the epidermis extracts measured by HPLC-MS/MS, it was not expected that the quantities would be completely equal but rather within the same range. However, no significant difference was found between the two methods. A difference in skin permeability was expected between the three different donors included in the study due to biological variation between individuals and skin sites. However, this was addressed by including skin from two donors for each of the three treatments. Hence it could be observed if one of the donated skin sites behaved oddly. However, even though arm skin is generally characterized as less permeable than abdominal skin [22] nothing indicated that the

permeability of the arm skin was lower than the abdominal skin from the other two included donors. In general, however, some variation is expected to be introduced by including the three donors and this was therefore tried to be addressed in figure 7 and 8 by indicating each biological replicate with a colour and shape for comparison of the HPLC-MS/MS and MALDI-qMSI results.

The MALDI-qMSI and HPLC-MS/MS analysis of the samples resulted in comparable quantitative amounts of tofacitinib. With MALDI-qMSI it was possible to detect local variations in the drug penetration together with endogenous molecules to visualize tissue attributes. The use of an acoustic microspotter for MALDI-qMSI has previously proven to enable absolute quantification in the epidermis in living skin equivalents and the application of the qMSI method is now further extended to the study of drug delivery to the epidermal compartment of human skin. This demonstrates that this method, with high probability, could be applied to any tissue model.

Previous experience has shown that manual deposition of droplets by pipettes resulted in variations in the deposited volume and the diameter of the droplet [1]. Here, the acoustic microspotter was used to create small reproducible droplets [9]. Acoustic microspotters may not be available in all MSI laboratories, but similar devices such as the Preddator automated spotter (<http://reddandwhyte.com>), which also handles nanoliter volumes have successfully been applied in other studies [23]. Besides the high reproducibility of the automated spotters, the small volumes make it possible to distinguish between compartments such as the epidermis and dermis which will, for instance, require a lot of tissue using the mimetic tissue model and larger areas would be required for manually spotted droplets onto control tissue.

In this study, epidermal concentrations of tofacitinib were of interest as its mode of action in the treatment of psoriasis is blockage of the STAT phosphorylation in the keratinocytes located in the epidermis [10]. Keratinocytes are known to undergo proliferation in stratum basale, an epidermal layer before they migrate and differentiate up through the epidermal layers until converted into corneocytes in the stratum corneum [24]. As the drug target is located in the epidermis, high skin retention and low skin permeation are attempted to enable STAT blockage in the epidermis and low systemic exposure. Therefore, as the C1 formulation was shown to retain tofacitinib in the skin it is considered likely that this formulation may provide a larger pool of tofacitinib near to target and hence result in a better bioavailability compared to the other formulations.

Different *in vitro* release profiles and *ex vivo* penetration and permeation profiles of tofacitinib were observed for the three formulations. IVRT addressed the differences in the release between the formulations and is usually implemented to describe quality changes or product sameness between formulation batches. The *ex vivo* skin penetration and permeation study predicted the drug uptake and permeation through the skin without describing factors such as clearance and metabolism which can only be investigated in *in vivo* studies [14,22]. This emphasizes that in order to optimise cutaneous drug delivery for the treatment of skin diseases, different techniques should be applied to increase the understanding of the complex interplay between the drug substance, the drug delivery systems and the properties of skin compartment(s) in scope for a specific drug target.

4 Conclusions

In this study, the drug delivery of tofacitinib was thoroughly explored in an IVRT setup and in an *ex vivo* skin penetration and permeation study using three different formulations where the permeation was studied using HPLC-MS/MS and the penetration using complementary analytical methods providing skin distribution analysis and quantification by MALDI-qMSI and HPLC-MS/MS.

The IVRT confirmed different release profiles for the three formulations where the highest flux was obtained for the aqueous gel and the lowest flux was obtained from C2. The *ex vivo* skin penetration and permeation study in human skin showed that the highest concentration of tofacitinib extracted from the skin was obtained with the samples treated with C1 whereas the greatest permeation of tofacitinib was observed for the samples treated with the aqueous gel. This demonstrates that interactions from the skin barrier influence the drug delivery of tofacitinib compared to the permeation over artificial membranes included in the IVRT study.

The MALDI-qMSI method used to quantify the epidermal concentrations in this study was developed for living skin equivalents but was successfully transferred to a more complex matrix, human skin. The linearity of the standard curves was improved by normalising the signal of tofacitinib to the signal of the IS compared to the signal of tofacitinib alone. Epidermal extracts analysed by HPLC-MS/MS showed similar results to the MALDI-qMSI analysis of the samples treated with C1. The skin distribution of tofacitinib visualized by MALDI-MSI showed that tofacitinib was primarily detected in the epidermis. The samples treated with the gel and C2 were below the LOQ using MALDI-qMSI except for a few particular regions. The study demonstrates that MALDI-qMSI is a promising method to

perform quantification and skin distribution investigations of the drug molecule and in regions where the concentration of the analyte was sufficient high, the skin distribution analysis made it possible to identify drug distribution and tissue features such as different compartments of the skin, hair follicles and sebaceous glands.

5 Acknowledgements

We thank Liselotte Saustrop Kirk and Anne-Louise Thomsen for expert technical assistance with bioanalysis of culture media and skin extracts and preparation of the formulations. We thank Cristina Russo, Nina Østergaard Knudsen, Rasmus Worm Mortensen, Mette Rydahl Sonne, André Huss Erikson, and Karen Lisbeth Høeg Lyngø for their expertise and technical input.

Full thickness human skin was sourced from healthy subjects following reconstructive surgery. All skin material was sampled in accordance with national legislation in the country of origin. The identities of the donors are not known to LEO Pharma and tissue was donated following informed written consent.

This work is partly funded by the Innovation Fund Denmark (IFD) under File No. 7038-00017B.

Declarations of interest: none

6 References

- [1] I. Rzagalinski, D.A. Volmer, Quantification of low molecular weight compounds by MALDI imaging mass spectrometry – A tutorial review, *Biochim. Biophys. Acta - Proteins Proteomics.* 1865 (2017) 726–739. <https://doi.org/10.1016/j.bbapap.2016.12.011>.
- [2] T. Porta, A. Lesur, E. Varesio, G. Hopfgartner, Quantification in MALDI-MS imaging: what can we learn from MALDI-selected reaction monitoring and what can we expect for imaging?, *Anal. Bioanal. Chem.* 407 (2015) 2177–2187. <https://doi.org/10.1007/s00216-014-8315-5>.
- [3] G. Hamm, D. Bonnel, R. Legouffe, F. Pamelard, J.-M. Delbos, F. Bouzom, J. Stauber, Quantitative mass spectrometry imaging of propranolol and olanzapine using tissue extinction calculation as normalization factor, *J. Proteomics.* 75 (2012) 4952–4961. <https://doi.org/10.1016/j.jprot.2012.07.035>.
- [4] C.W. Chumbley, M.L. Reyzer, J.L. Allen, G.A. Marriner, L.E. Via, C.E. Barry, R.M. Caprioli, Absolute Quantitative MALDI Imaging Mass Spectrometry: A Case of Rifampicin in Liver Tissues, *Anal. Chem.* 88 (2016) 2392–2398. <https://doi.org/10.1021/acs.analchem.5b04409>.
- [5] D.A. Pirman, A. Kiss, R.M.A. Heeren, R.A. Yost, Identifying Tissue-Specific Signal

- Variation in MALDI Mass Spectrometric Imaging by Use of an Internal Standard, *Anal. Chem.* 85 (2013) 1090–1096. <https://doi.org/10.1021/ac3029618>.
- [6] D.A. Pirman, R.F. Reich, A. Kiss, R.M.A. Heeren, R.A. Yost, Quantitative MALDI Tandem Mass Spectrometric Imaging of Cocaine from Brain Tissue with a Deuterated Internal Standard, *Anal. Chem.* 85 (2013) 1081–1089. <https://doi.org/10.1021/ac302960j>.
- [7] M.R. Groseclose, S. Castellino, A Mimetic Tissue Model for the Quantification of Drug Distributions by MALDI Imaging Mass Spectrometry, *Anal. Chem.* 85 (2013) 10099–10106. <https://doi.org/10.1021/ac400892z>.
- [8] J.A. Barry, R. Ait-Belkacem, W.M. Hardesty, L. Benakli, C. Andonian, H. Licea-Perez, J. Stauber, S. Castellino, Multicenter Validation Study of Quantitative Imaging Mass Spectrometry, *Anal. Chem.* 91 (2019) 6266–6274. <https://doi.org/10.1021/acs.analchem.9b01016>.
- [9] C. Russo, N. Brickelbank, C. Duckett, S. Mellor, S. Rumbelow, M.R. Clench, Quantitative Investigation of Terbinafine Hydrochloride Absorption into a Living Skin Equivalent Model by MALDI-MSI, *Anal. Chem.* 90 (2018) 10031–10038. <https://doi.org/10.1021/acs.analchem.8b02648>.
- [10] D.M. Schwartz, Y. Kanno, A. Villarino, M. Ward, M. Gadina, J.J. O’Shea, JAK inhibition as a therapeutic strategy for immune and inflammatory diseases, *Nat. Rev. Drug Discov.* 17 (2017) 78. <https://doi.org/10.1038/nrd.2017.267>.
- [11] K. Ghoreschi, M. Gadina, Jakpot! New small molecules in autoimmune and inflammatory diseases, *Exp. Dermatol.* 23 (2014) 7–11. <https://doi.org/10.1111/exd.12265>.
- [12] K.A. Papp, M.A. Menter, M. Abe, B. Elewski, S.R. Feldman, A.B. Gottlieb, R. Langley, T. Luger, D. Thaci, M. Buonanno, P. Gupta, J. Proulx, S. Lan, R. Wolk, Tofacitinib, an oral Janus kinase inhibitor, for the treatment of chronic plaque psoriasis: results from two randomized, placebo-controlled, phase III trials, *Br. J. Dermatol.* 173 (2015) 949–961. <https://doi.org/10.1111/bjd.14018>.
- [13] U.S Department of Health and Human Services, Center for Drug Evaluation and Research, SUPAC-SS: Nonsterile Semisolid Dosage Forms; Scale-Up and Post-Approval Changes: Chemistry, Manufacturing and Controls; In Vitro Release Testing and In Vivo Bioequivalence Documentation | FDA, SUPAC-SS. (1997). <https://www.fda.gov/regulatory-information/search-fda-guidance-documents/supac-ss-nonsterile-semisolid-dosage-forms-scale-and-post-approval-changes-chemistry-manufacturing> (accessed March 5, 2020).
- [14] L. Raghavan, M. Brown, B. Michniak-Kohn, S. Ng, S. Sammeta, In Vitro Release Tests as a Critical Quality Attribute in Topical Product Development, in: N. Langley, B. Michniak-Kohn, D.W. Osborne (Eds.), *Role Microstruct. Top. Drug Prod. Dev.*, Springer International Publishing, Cham, 2019: pp. 47–87. https://doi.org/10.1007/978-3-030-17355-5_2.
- [15] P. Källback, A. Nilsson, M. Shariatgorji, P.E. Andrén, MsIQuant - Quantitation Software for Mass Spectrometry Imaging Enabling Fast Access, Visualization, and Analysis of Large Data Sets, *Anal. Chem.* 88 (2016) 4346–4353. <https://doi.org/10.1021/acs.analchem.5b04603>.

- [16] P. Källback, M. Shariatgorji, A. Nilsson, P.E. Andrén, Novel mass spectrometry imaging software assisting labeled normalization and quantitation of drugs and neuropeptides directly in tissue sections, *J. Proteomics*. 75 (2012) 4941–4951. <https://doi.org/https://doi.org/10.1016/j.jprot.2012.07.034>.
- [17] J. D'Alvise, R. Mortensen, S.H. Hansen, C. Janfelt, Detection of follicular transport of lidocaine and metabolism in adipose tissue in pig ear skin by DESI mass spectrometry imaging, *Anal. Bioanal. Chem.* 406 (2014) 3735–3742. <https://doi.org/10.1007/s00216-014-7802-z>.
- [18] J.A. Barry, M.R. Groseclose, S. Castellino, Quantification and assessment of detection capability in imaging mass spectrometry using a revised mimetic tissue model, *Bioanalysis*. 11 (2019) 1099–1116. <https://doi.org/10.4155/bio-2019-0035>.
- [19] A.M. Handler, M. Fallah, A. Just Pedersen, G. Pommergaard Pedersen, K. Troensegaard Nielsen, C. Janfelt, MALDI mass spectrometry imaging as a complementary analytical method for improved skin distribution analysis of drug molecule and excipients, *Int. J. Pharm.* 590 (2020) 119949. <https://doi.org/https://doi.org/10.1016/j.ijpharm.2020.119949>.
- [20] D. Bonnel, R. Legouffe, A.H. Eriksson, R.W. Mortensen, F. Pamelard, J. Stauber, K.T. Nielsen, MALDI imaging facilitates new topical drug development process by determining quantitative skin distribution profiles, *Anal. Bioanal. Chem.* 410 (2018) 2815–2828. <https://doi.org/10.1007/s00216-018-0964-3>.
- [21] I.S. Sørensen, C. Janfelt, M.M.B. Nielsen, R.W. Mortensen, N. Knudsen, A.H. Eriksson, A.J. Pedersen, K.T. Nielsen, Combination of MALDI-MSI and cassette dosing for evaluation of drug distribution in human skin explant, *Anal. Bioanal. Chem.* 409 (2017) 4993–5005. <https://doi.org/10.1007/s00216-017-0443-2>.
- [22] R.C. Wester, H.I. Maibach, Regional Variation in Percutaneous Penetration, in: R.L. Bronaugh, H.I. Maibach (Eds.), *Percutaneous Absorpt. Drugs-Cosmetics-Mechanisms-Methodology*, 3rd ed., Marcel Dekker, Inc., New York, NY, 1999: pp. 107–116.
- [23] T. Vallianatou, N. Strittmatter, A. Nilsson, M. Shariatgorji, G. Hamm, M. Pereira, P. Källback, P. Svenningsson, M. Karlgren, R.J.A. Goodwin, P.E. Andrén, A mass spectrometry imaging approach for investigating how drug-drug interactions influence drug blood-brain barrier permeability, *Neuroimage*. 172 (2018) 808–816. <https://doi.org/https://doi.org/10.1016/j.neuroimage.2018.01.013>.
- [24] J. van Smeden, M. Janssens, G.S. Gooris, J.A. Bouwstra, The important role of stratum corneum lipids for the cutaneous barrier function, *Biochim. Biophys. Acta - Mol. Cell Biol. Lipids*. 1841 (2014) 295–313. <https://doi.org/https://doi.org/10.1016/j.bbalip.2013.11.006>.

Tables

Table 1. Physicochemical properties of tofacitinib.

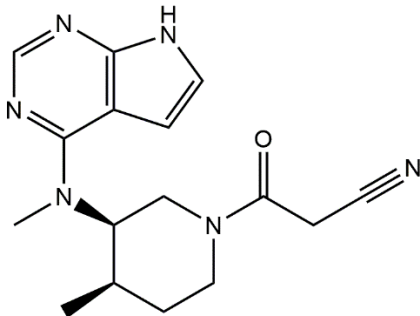
Physicochemical properties of tofacitinib	
Molecular structure	
Sum formula	C ₁₆ H ₂₀ N ₆ O
Monoisotopic mass	312.1699
Log D (pH=7.4)	1.9 [21]
pKa	1.6 and 5 [21]

Table 2. Flux presented as mean \pm SD (n=6) along with lag time, amount released after 6 hours and the linear fit, R².

	Treatment		
	Gel	C1	C2
Flux ($\mu\text{g}/(\text{min}^{1/2} \text{ cm}^2)$)	90.9 \pm 8.0	56.8 \pm 7.8	32.2 \pm 2.9
Lag time (min)	11	18	5
Released after 6 h ($\mu\text{g cm}^{-2}$)	1459 \pm 103	886 \pm 60	563 \pm 59
R ²	0.99	0.98	0.99

Figures

Figure 1. The amount tofacitinib in the receptor compartment per area ($\mu\text{g}/\text{cm}^2$) depicted as a function of the square root of time ($\text{min}^{1/2}$) (n=6).

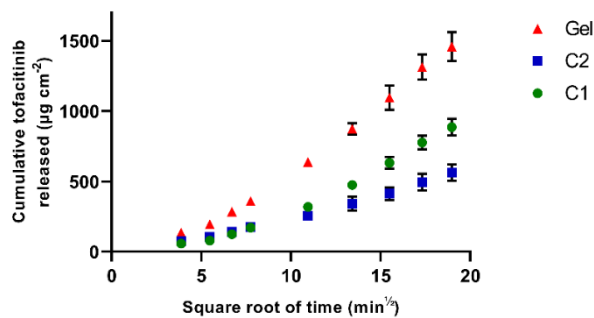


Figure 2. a) Penetration of tofacitinib in epidermis shown in magenta and dermis shown in black at 5 hours (upper panel) and 24 hours (lower panel). At 5 hours, the total content of tofacitinib in the skin is statistically different between the samples treated with C1 or the gel ($p=0.0338$). Similar to the 5-hour samples, a statistical difference was again found between the samples treated with C1 and gel after 24 hours ($p=0.0219$). b) The permeated amount of tofacitinib is shown after 24 hours. Tofacitinib was only detected in one cell for the samples treated with C1 after 24 hours. The samples below LOQ are presented as zero. The horizontal lines show the mean values, and * indicates a statistically significant difference $p \leq 0.05$.

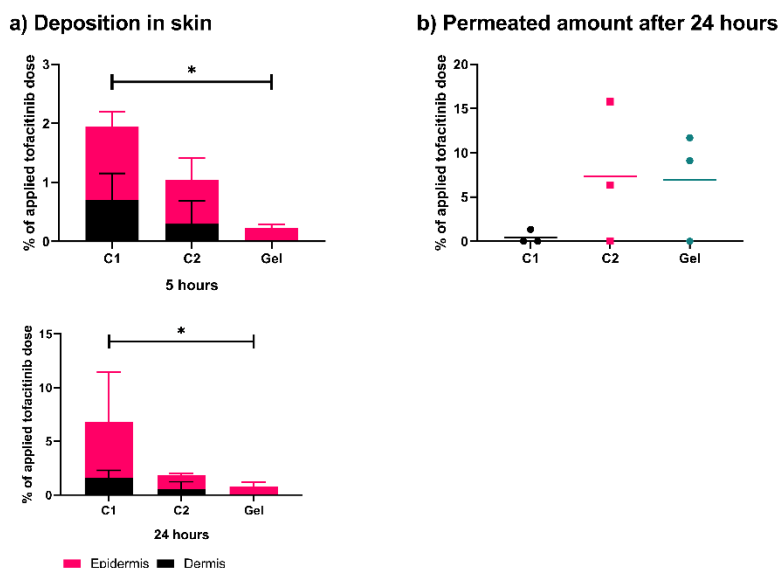


Figure 3. H&E stained cross-section and MALDI images of the epidermal marker and spots of IS using bicubic interpolation. In the bottom, an overlay of the ion images of the epidermal marker in green and IS in red is presented using the nearest neighbour interpolation.

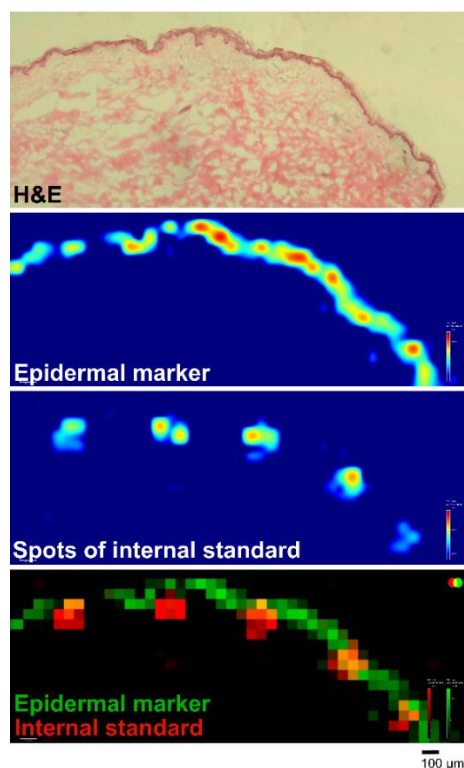
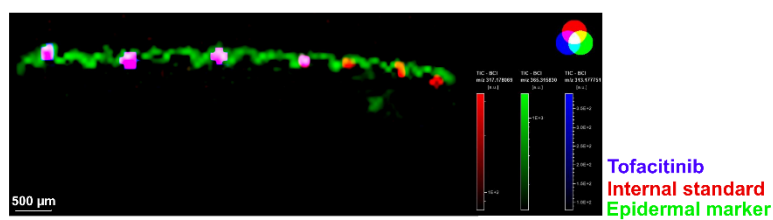
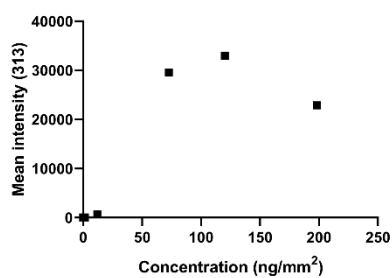


Figure 4. a) MALDI image of microspotted calibration standards, b) the mean intensity of tofacitinib and c) the mean intensity ratio of tofacitinib and IS plotted as a function of the concentration of tofacitinib (ng/mm^2) including the 95 % confidence band. The linear regression for the mean intensity ratio is described as; mean intensity ratio = $0.0813[\text{tofacitinib}] + 0.184$ with a linear fit of $R^2 = 0.996$.

a) MALDI image of microspotted standards



b) Without normalization



c) Normalized

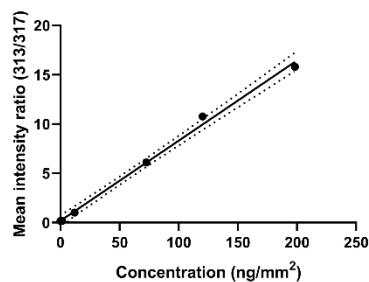
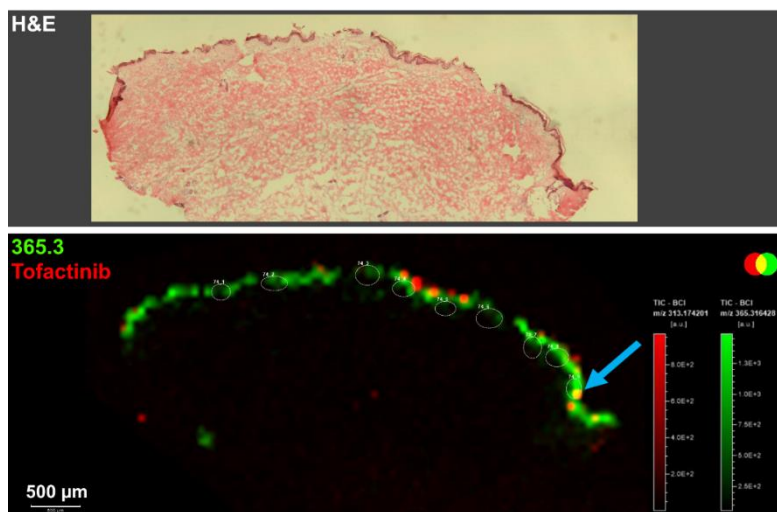


Figure 5. H&E stained tissue and overlay of ion images showing the epidermal marker 365.3 in green and tofacitinib in red. a) Skin cross-section treated with C2 cream and b) treated with gel. Arrows marks spots above LOQ.

a) C2



b) Gel

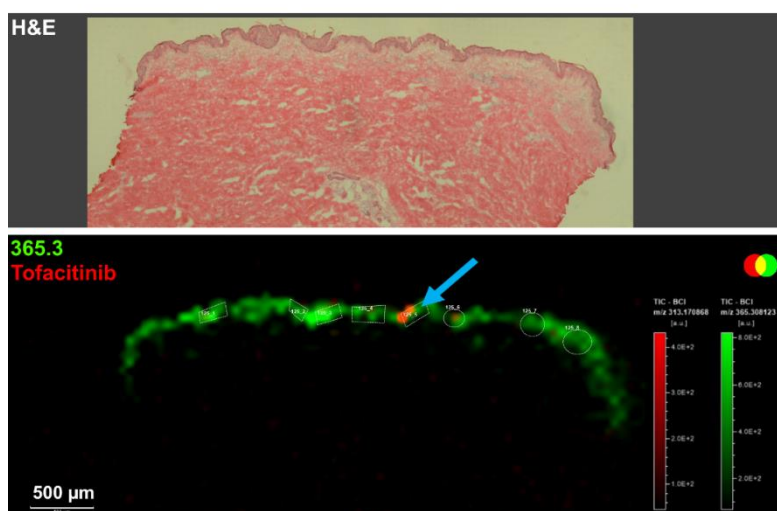
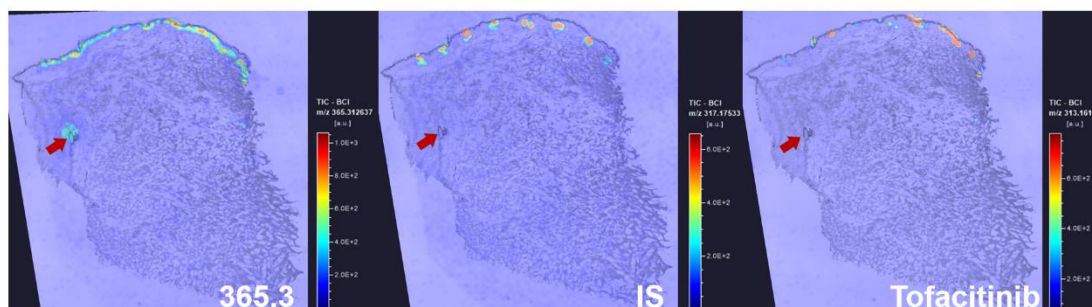


Figure 6. Cross-section of skin treated with tofacitinib in C1 cream for a) 5 and b) 24 hours. For each of the two cross-sections of skin a MALDI image of the epidermal marker, spots of the IS and tofacitinib in the epidermis and upper dermis. The MALDI images are overlaid by the H&E stain. Hair follicles were marked by an arrow.

a) 5 hours



b) 24 hours

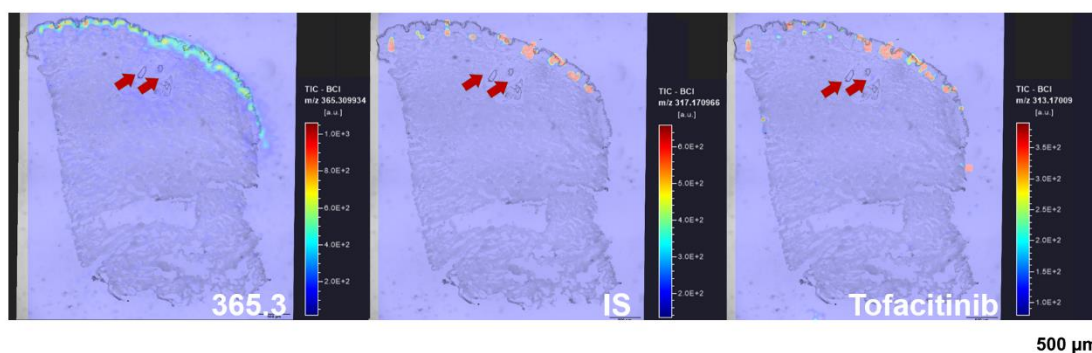


Figure 7. Concentrations (ng/mm^2) of the individual microspotted epidermal spots are shown for each biological replicate. The concentrations shown are not corrected with the contribution of the non-labelled impurity from the IS. The magenta coloured points mark the 24-years old donor and the black the 62-years old woman. Some samples had fewer than nine spots due to the spots not aligned with the epidermis. The alignment of the spots was checked using the epidermal marker at m/z 365.3. The horizontal line for each biological replicate indicates the mean value.

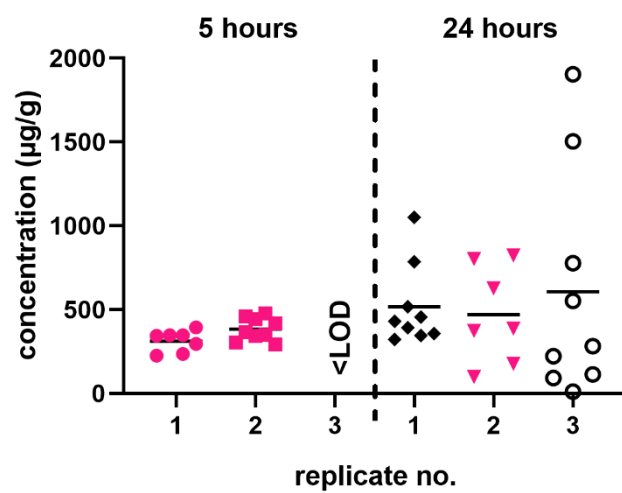


Figure 8. Comparison of the quantitation of tofacitinib in the epidermis by MALDI-qMSI and HPLC-MSMS. The magenta coloured marks the 24-years old donor and the black the 62-years old woman. The dots, cubes and squares are used to distinguish the individual samples and the shapes match the shape of the samples shown in figure 7. No statistical difference was found between the two methods at 24 hours ($p=0.70$).

